24th COBEM - 2017

24th ABCM International Congress of Mechanical Engineering
December 3-8, 2017, Curitiba, PR, Brazil

COBEM-2017-2141
EXPERIMENTAL EVALUATION OF THERMAL INSTABILITIES DURING FLOW BOILING OF DI-WATER IN MICROCHANNELS HAVING THEIR SURFACES COVERED WITH NANOPARTICLES

Tiago Augusto Moreira[1)]
Francisco Júlio do Nascimento[2)]
Gherhardt Ribatski[3)]
Heat Transfer Research Group, Escola de Engenharia de São Carlos (EESC), University of São Paulo (USP), Av. Trabalhador São-Carlense, 400, Parque Arnold Schimidt, CEP: 13566-590, São Carlos, Brazil.
[1)]tiago.moreira@usp.br
[2)]fnascimento@sc.usp.br
[3)]ribatski@sc.usp.br

Abstract. *The present paper concerns an experimental evaluation of the influence of nanoparticles deposition inherent to the boiling process of nanofluids on thermal instabilities during flow boiling of DI-water inside a single microchannel (1.1 mm ID and 200 mm long). Experiments were performed for tubes as commercially available and with their surfaces covered with Al_2O_3 nanoparticles (20-30 and 40-80 nm), and SiO_2 (15 and 80 nm). The surface coating was obtained by submitting the test section to a boiling process of nanofluids with volumetric concentration of 0.1%. Thermal instabilities were characterized by the amplitude of the temperature oscillations of the DI-water at the channel inlet. In general, surfaces covered with nanoparticles smaller than 30 nm provide a reduction of thermal instability effects. For larger nanoparticles, an opposite behavior was noted and higher thermal instabilities were observed compared to flow boiling of DI-water on the original surface. An analysis of the tubes surfaces was performed in order to evaluate the effect of deposition on the surface texture and, consequently, on the density of bubble nucleation sites. It was found that the deposition of nanoparticles smaller than 30 nm provides a reduction of the number of cavities with sizes within the range of dimensions corresponding to active nucleation sites, relative to the surface as commercially evaluated. This behavior was associated to the reduction of thermal instability effects. An opposite trend was observed for nanoparticles larger than 40 nm.*

Keywords: *Flow boiling, Nanofluids, Microchannels, Thermal instabilities.*

1. INTRODUCTION

The addition of nanoparticles to a base fluid to improve its transport properties and, consequently, the heat transfer coefficient in single-phase heat transfer processes was firstly proposed by Choi and Eastman (1995). In the same study, as far as the present authors known, Choi and Eastman (1995) were also the first to name as nanofluids solutions composed of nanoparticle and a base fluid. Since then, the number of studies involving nanofluids increased considerably, opening new research paths focusing also on the stability of nanofluids, the characterization of these suspensions and the use of them in pool and flow boiling processes.

It is well known in literature (Wen *et al*., 2011; Diao *et al*., 2013; Souza *et al*., 2014) that the boiling process of nanofluids on a surface promotes the deposition of nanoparticles on it, affecting the bubble nucleation, growing and departure processes. Xu and Xu (2012) and Yu *et al*. (2015) observed a reduction of the flow thermal instabilities, characterized by the variation of the amplitude of fluid temperature oscillations at the inlet of the test section, by performing experiments for flow boiling of nanofluids. Those authors associated such behavior to the reduction of bubbles departure diameter with decreasing the surface tension associated to the addition of nanoparticles. They also noted the reduction of back flow intensity due to bubble expansion for flow boiling of nanofluids compared to the respective base fluids.

In the present study, flow boiling experiments were performed for DI-water inside microchannels having their internal surfaces previously covered with nanoparticles to evaluate if the reduction of temperature oscillations of the test fluid at the channel inlet is associated to modifications of surface texture. Initially, the internal surface of the microchannels were covered with nanoparticles through flow boiling processes. Then, after this procedure, tests for

flow boiling of DI-water were performed. The effect of deposition of two sizes of Al_2O3 (20-30 and 40-80 nm) and two sizes of SiO_2 (15 and 80 nm) were evaluated. Analyses of the internal surface of the tubes through images obtained with a Vecco Wiko optical profiler (10x magnification) were performed before and after the tests with DI-water to evaluate the modification of the surface texture, and its effect on the transient behavior of the fluid temperature at the microchannel inlet.

2. EXPERIMENTAL APPARATUS AND PROCEDURES

In this section, detailed descriptions of the experimental apparatus and procedures are presented.

2.1 Experimental facility

Figure 1 illustrates the experimental apparatus and details of the test section. In the facility, the test fluid is driven from the reservoir through the circuit by a gear pump (Micropump GA-T23). The mass flow rate is estimated from single-phase pressure drop measurements through a 2.0 mm ID, 100 mm long quartz tube using a differential pressure transducer (Endress+Hauser PMD75) with a measurement span of 0-3 kPa. Calibration curves were previously adjusted correlating the pressure drop and mass flow rate using as reference the mass deposition in a digital analytical balance (precision of 0.01 g). During this procedure, the facility was runed as an open circuit. Such in-house made measuring device was used to avoid possible effects on the flow rate measurements of nanoparticles deposition on the internal parts of commercial and non-internally inspectable flow meters. The error associated with the mass flow meter was found equal to 4.6% of the measured value with reliability of 95.4%. Details of the mass flow meter are presented in Moreira (2017).

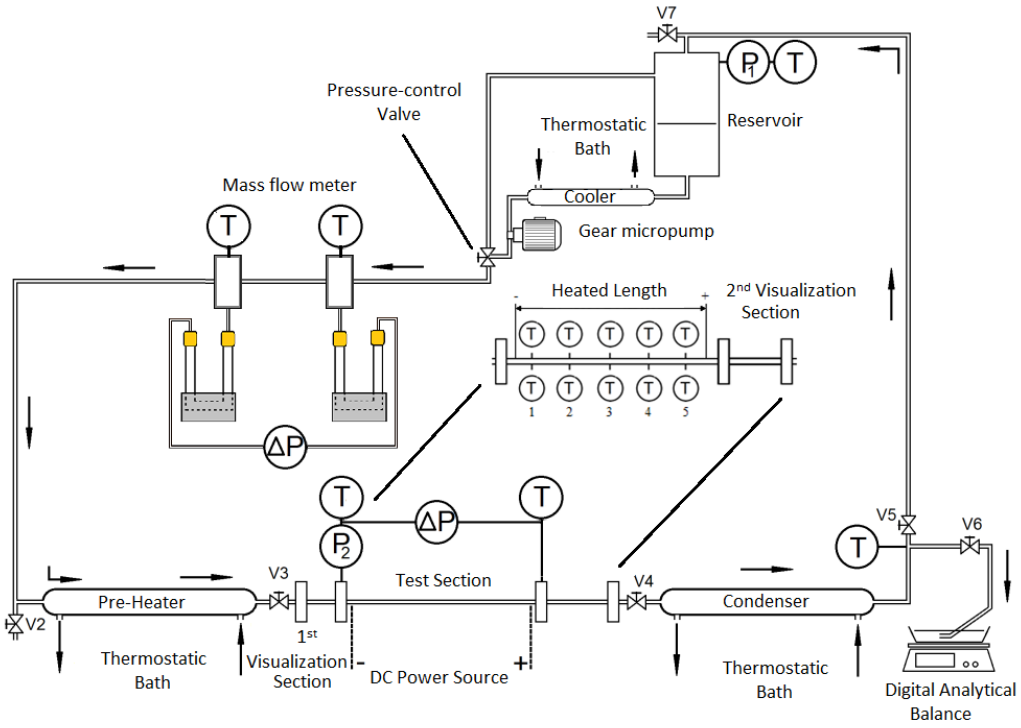

Figure 1. Schematic of the test facility.

A pre-heater consisting of a tube-in-tube heat exchanger was used to impose the inlet temperature of the test fluid at the test section inlet. This heat exchanger used as heating source a thermal fluid (capable of working at temperatures up to 317°C) whose temperature is controlled by a thermal bath. Needle valves located upstream and downstream of the test section were used to minimize two-phase flow oscillations due to the confined bubble formation. Therefore, variations of the intensity of fluid temperature oscillations can be attributed only to changes in the phenomenology of the flow boiling process. At the test section entrance, measurements of bulk temperature, using a thermocouple positioned within the flow, and absolute pressure, using a pressure transducer (Endress+Hauser PMP131 for 0-400 kPa) were performed. The pressure drop along the test section was evaluated through a differential pressure transducer

(Endress+Hauser PMD75 for 0-300 kPa). The outlet temperature was measured through a thermocouple positioned within the flow.

The test section is a stainless-steel tube (AISI-304) with internal diameter of 1.1 mm and 200 mm long. The heating effect on the test section was obtained by supplying electrical current from a DC power source (TDK-Lambda GEN 20V-76A) directly to the test surface. Measurements of temperature were performed in 5 cross sections of the test tubes, as illustrated in Fig. 1. These sections were numbered from 1 to 5 starting from the inlet of the duct. All temperatures were measured by K-type thermocouples with hot junction diameters of 0.152 mm. Just downstream of the test section was a 1.0 mm ID and 100 mm long quartz tube, installed in order to allow two-phase flow visualizations with a high-speed camera. Downstream the transparent tube was a heat exchanger (condenser) responsible to condense and subcool the test fluid by rejecting heat to a secondary fluid which temperature is controlled by a second thermal bath. The condenser, the pre-heater, the flow meter and the reservoir are made of borosilicate glass, allowing the evaluation of deposition of nanoparticles along the circuit. To record the data and to monitor and control the experimental apparatus, a LabView program was used with a National Instruments data acquisition system (SCXI-1000 with SCXI-1102 thermocouples module).

The test facility and the data regression procedure were validated through comparisons of heat transfer and pressure drop experimental results for single-phase flow and well-established prediction methods from literature (see Moreira et al., 2017).

2.2 Experimental procedure

The surfaces coating was obtained by boiling nanofluids with volumetric concentration of 0.1% internally to the test tube. For the coating (deposition), the nanofluids were inserted in the experimental apparatus, boiled along the test section, and then withdrawn.

Experiments to evaluate the oscillations of the fluid inlet temperature were performed for the following conditions: (i) DI-water for the tube surface as received from the manufacturer (BBN); and (ii) DI-water on the coated surface for depositions obtained with nanoparticles volumetric concentration of 0.1% (ABN 0.1%).

Firstly, the DI-water (working fluid) was boiled in an open vessel for a period of 30 minutes in order to eliminate non-condensable gases. Then, the experimental apparatus was evacuated down to an absolute pressure of 10 kPa, and then charged with the boiling DI-water. The tests were performed for a saturation temperature at the test section outlet of 102 ± 3°C, subcooling at the test section inlet of 25°C, heat fluxes ranging from 100-350 kW/m^2, vapor quality at the test section outlet from 0.01 to 0.5 and mass velocities of 200, 400 and 600 kg/m^{2}s.

The nanofluids were prepared according to the two-steps method, which consists of adding nanoparticles, weighed through a digital analytical balance, to a base fluid (DI-water) and dispersing them through ultrasonication during a period of 30 minutes (Coleparmer CP505). Once prepared, the nanofluid was loaded into the test facility.

Temperature measurements were calibrated and their uncertainties were evaluated according to the procedure suggested by Abernethy and Thompson (1973). The uncertainties of the pressure transducers and the power supplier were determined based on the data provided by the manufacturers. Table 1 shows the experimental uncertainties.

Table 1. Experimental uncertainties.

Parameter	Uncertainty
D	20 μm
L	1 mm
p	4.5 kPa
Δp	225 Pa
G	4.6%
T	0.15°C
Q	0.8
ω*	1%
Heated length	1 mm
x	0.001

*of the expected volumetric concentration

3. RESULTS

For DI-water tests with the surface without deposition (DI-water BBN), it was found that the thermal instability effects increase with increasing the heat flux and mass velocity. This behavior is illustrated in Fig. 2, which shows the variations of the temperature of the test fluid at the test section inlet, T_{inlet}. Similar behavior was observed for the surfaces covered with Al_2O_3 (20-30 nm) and Al_2O_3 (40-80 nm), as seen in Fig 3. On the other hand, for SiO_2 nanoparticles with diameter of 15 nm, the effects of heat flux and mass velocity on the intensity of thermal instabilities

were found negligible. For SiO_2 nanoparticle with dimensions of 80 nm, the amplitude of the oscillations of the fluid inlet temperature rises marginally and their frequency decreases with increasing heat flux and mass velocity, as illustrated in Fig. 4.

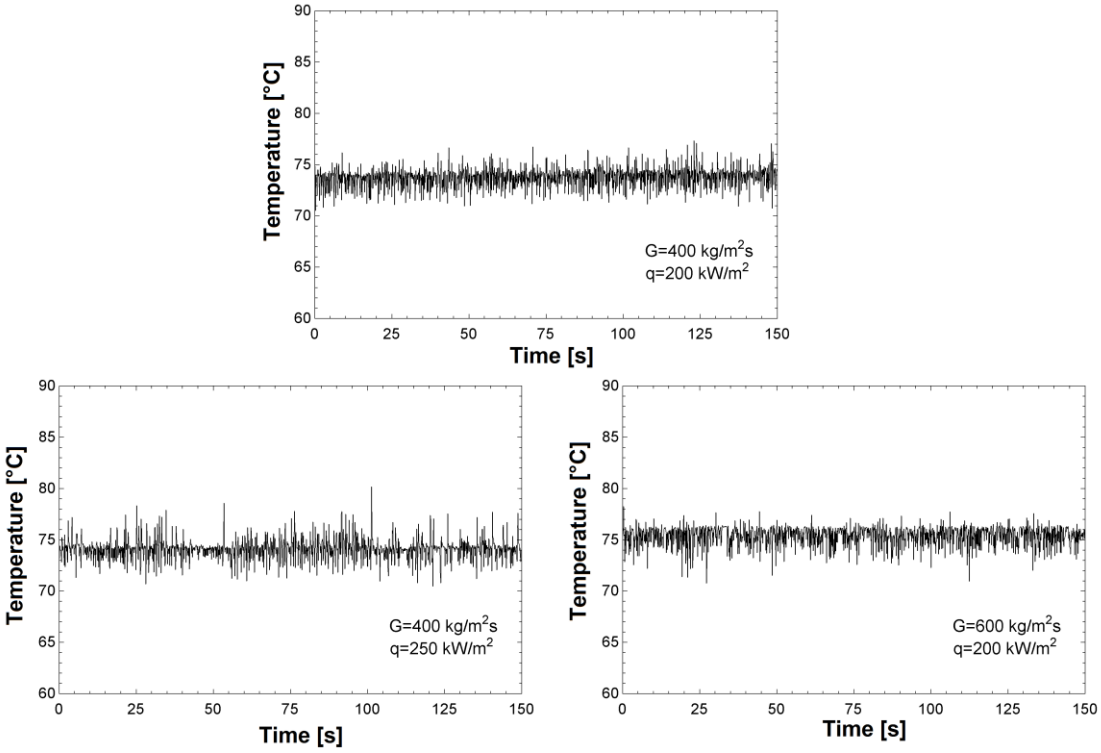

Figure 2. Temperature oscillations of the fluid at the test section inlet for the original surface.

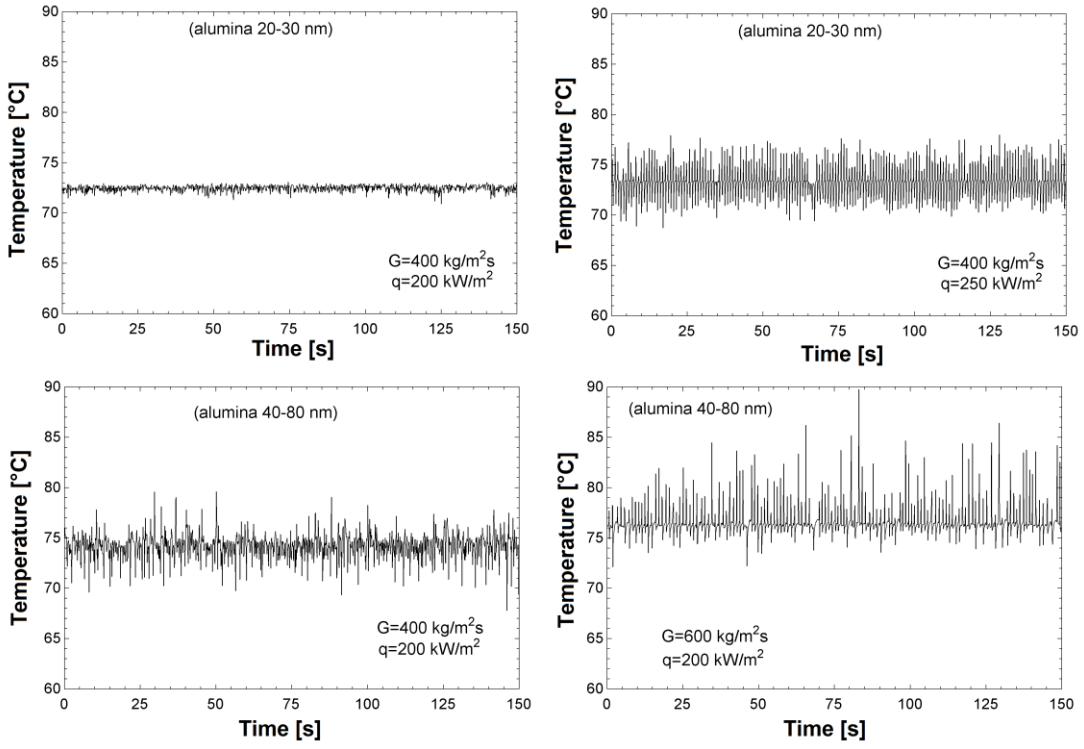

Figure 3. Effect of heat flux and mass velocity on the inlet temperature oscillations of the test fluid for the surfaces covered with Al_2O_3 (20-30 nm) and Al_2O_3 (40-80 nm).

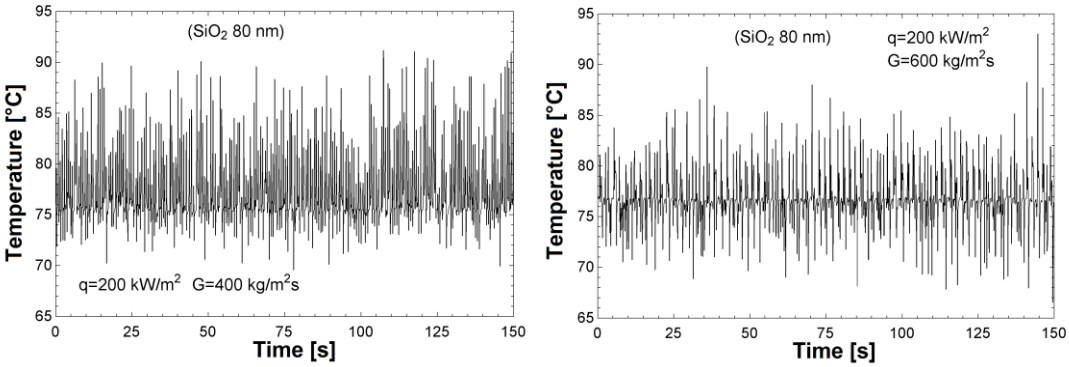

Figure 4. Effect of heat flux and mass velocity on the inlet temperature oscillations of the test fluid for the surfaces covered with SiO_2 80 nm.

Figure 5 illustrates the transient behavior of the temperature of the test fluid for G=400 kg/m^{2}s and q=200 kW/m^2 at the test section inlet T_{inlet} for the surfaces evaluated in the present study. In this figure, it can be noted that the amplitude of the oscillations of T_{inlet} is lower for the surfaces covered with nanoparticles smaller than 30 nm, independently of their material. Surfaces covered with nanoparticles larger than 40 nm presented higher T_{inlet} oscillations associated to thermal instability effects.

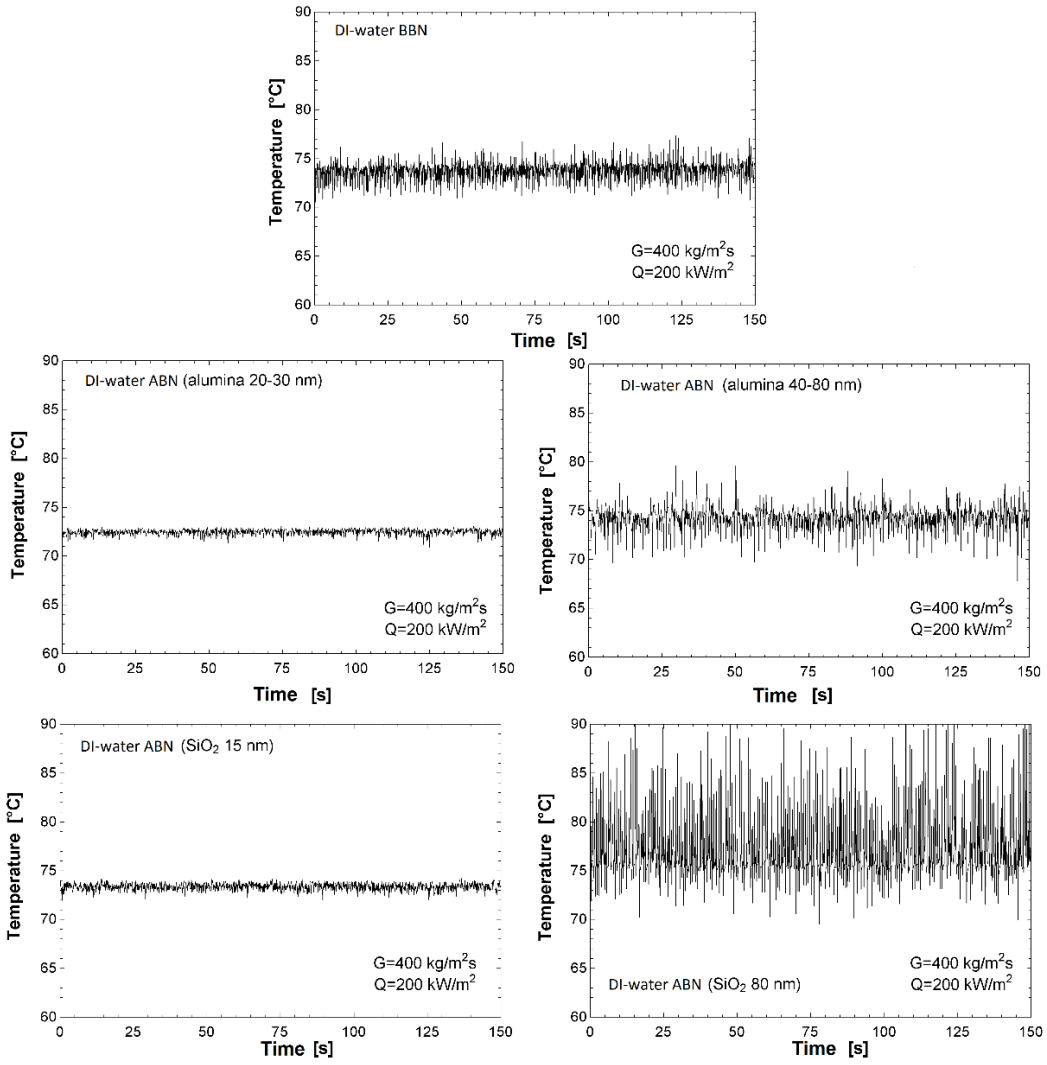

Figure 5. Temperature oscillations of the fluid at the test section inlet.

The thermal instabilities characterized by variations of the fluid temperature at the test section inlet are intrinsically related to the bubble expansion inside small diameter channels under confined conditions. Due to the reduced dimension of the channel, the bubble growth provides a significant backforce against the flow. This effect is enhanced for low pressure fluids like water, which present high liquid-to-vapor density ratio. Therefore, the bubbles grow rapidly in both directions, downstream and upstream, during their expansion before their detachment. Under these circumstances, it is possible to speculate that the forces associated to the bubble growing process at each bubble nucleation are summed. Thus, as higher the number of active nucleation sites, greater the backflow effects and, consequently, thermal instability effects. So, in order to explain the results displayed in Fig. 5, a surface analysis was performed evaluating the possible effect of the deposition on the density of active sites of bubble nucleation.

Figure 6 illustrates images of the texture of the internal surfaces with and without deposition obtained through an optical profiler from VeccoWiko model NT1100 with magnification of 10 times. From these images, it can be noted different deposition patterns depending on the size of the nanoparticle. The larger ones ($40<d_p<80$ nm) promote an almost uniform deposition, becoming the covered surface similar to the surface as commercially evaluated. The opposite occurs for the smaller nanoparticles, where the deposition is clearly non-uniform, presenting regions of peaks and valleys.

Although relationships can be found between the roughness parameters and the characteristics of the cavities on the surface, it is well known that bubble nucleation process is mainly affected by the cavity radius and not by its deepness (Collier and Thome, 1994). So, instead of working with the roughness parameters, it was performed a spatial Power Spectrum Density (PSD) analysis of the distribution of the radius of the cavities on the surfaces.

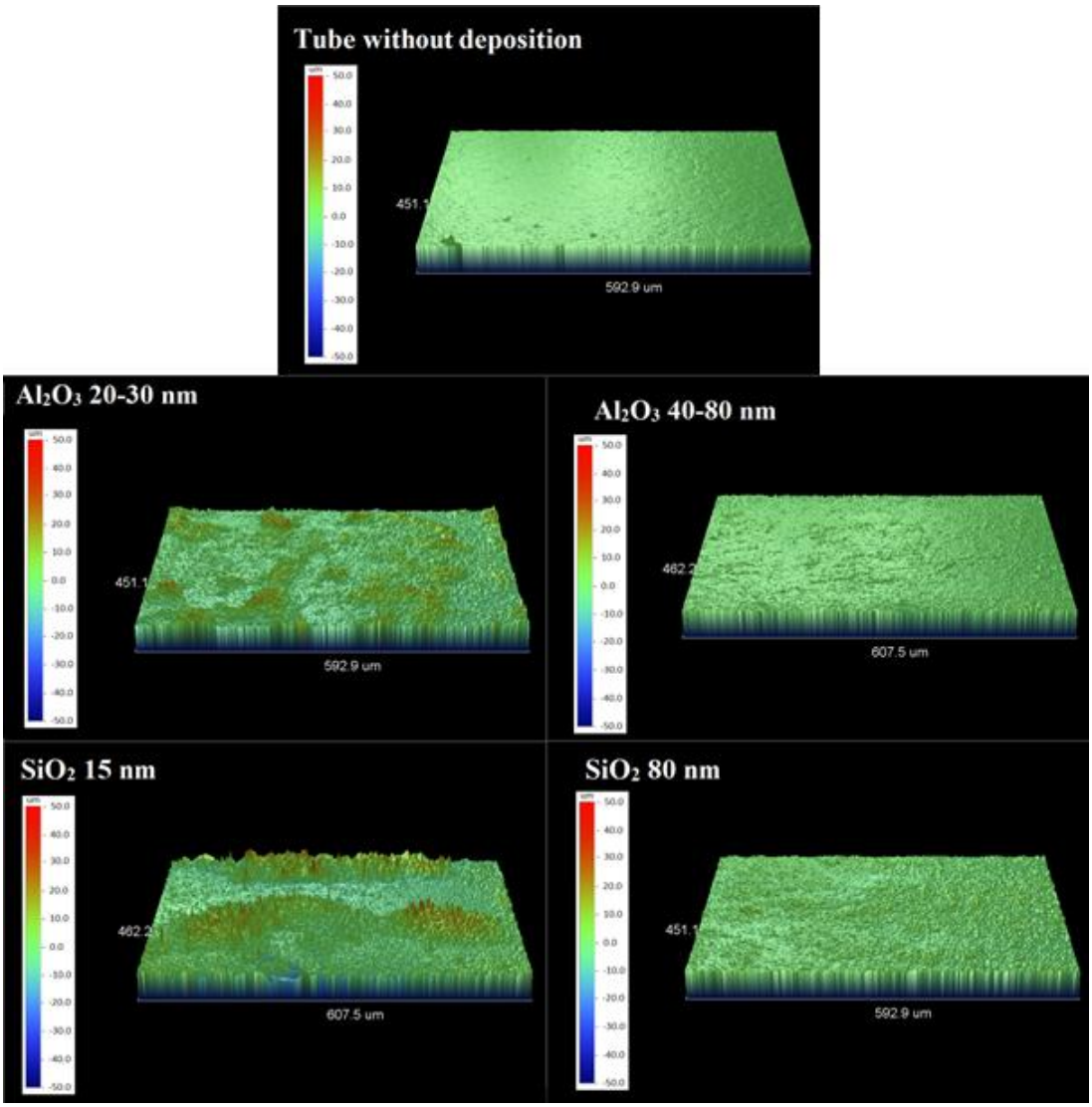

Figure 6. Images obtained for the surfaces through an optical profiler.

In Fig. 7, the results for the PSD were normalized by dividing the PSD value corresponding to each spatial frequency by the integral of the Power Spectrum Density distribution. The values of maximum and minimum radius of active nucleation cavities according to the criterion of Kandlikar *et al.* (1997) are also given in Fig. 7 as a function of the receding contact angle.

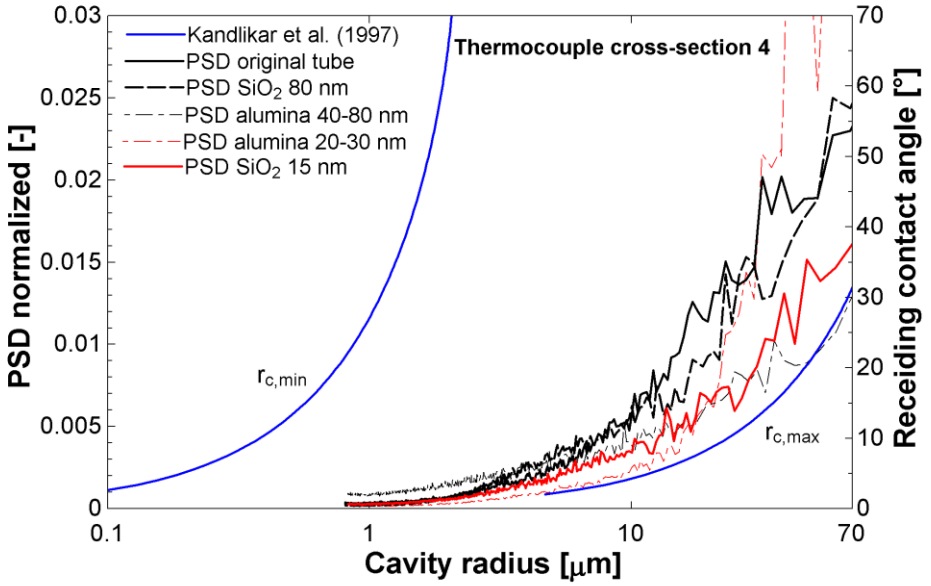

Figure 7. Comparison of the PSD curves and the Kandlikar *et al*. (1997) criterion ($r_{c,min}$ and $r_{c,max}$ are respectively the minimum and maximum radius of bubble nucleation as function of the contact angle).

Table 2 presents the areas of the PSDs limited by the Kandlikar *et al.* (1997) criterion for the surfaces obtained through the deposition process and the original one considering receding contact angles of 15° and 20°, respectively, values commonly observed in the literature for DI-water (Forrest *et al.*, 2010). It is worth to highlight that the number of cavities comprised by the range of dimensions corresponding to active nucleation sites increases according to the areas of the PSDs. According to Tab. 2, it is noted that the number of cavities within the range corresponding to active nucleation sites are considerably lower for the surfaces covered with the smaller nanoparticles than for the tube as commercially available. Considering the larger nanoparticles, none significant difference was seen between the PSDs areas of the original tube and the surfaces covered with nanoparticles. Moreover, under certain conditions as for the deposition of Al_2O_3 (40-80 nm) and the first three cross sections containing thermocouples, the PSDs areas for the deposited surface are slightly higher than for the original tube.

Table 2. Integral of the normalized PSD limited by the criterion of Kandlikar *et al*. (1997).

Receding contact angle [°]	Thermocouple cross-section*	Tube as received	Al_2O_3 20-30 nm	Al_2O_3 40-80 nm	SiO_2 15 nm	SiO_2 80 nm
15	1	0.74	0.27	0.87	0.69	0.77
	2	0.74	0.36	0.86	0.52	0.70
	3	0.74	0.37	0.86	0.66	0.78
	4	0.74	0.17	0.72	0.61	0.81
	5	0.74	0.37	0.63	0.75	0.84
20	1	0.82	0.33	0.90	0.74	0.84
	2	0.82	0.49	0.90	0.56	0.77
	3	0.82	0.48	0.89	0.73	0.84
	4	0.82	0.21	0.81	0.68	0.87
	5	0.82	0.42	0.72	0.80	0.88

*from the beginning of the test section (see Fig. 1)

The comparison of the distribution of sizes of cavities on the surface and the criterion of Kandlikar *et al*. (1997) for bubble nucleation under convective boiling conditions inside microchannels, illustrated in Fig. 7 and Tab. 2,

corroborates the results observed by Xu and Xu (2015) and Yu *et al*. (2015) and the ones displayed in Fig. 5, which relates changes in the thermal instabilities of the flow to the deposition of nanoparticles on the wall. From this comparison, it can be concluded that the deposition of nanoparticles smaller than 30 nm implied on the reduction of the density of active nucleation sites on the surface, as seen in Tab. 2, and on the reduction of the thermal instabilities of the flow, as observed in Fig. 5. On the other hand, for nanoparticles larger than 40 nm, Tab. 2 shows that the deposition almost did not affect the density of active nucleation sites in relation to the bare tube, and a slight increase in the amplitude of the inlet temperature oscillations relative to the original surface was seen in Fig. 5.

It can be speculated that the reduction of the density of cavities within the range of active nucleation sites observed for the surfaces covered with the smaller nanoparticles (d_p<30 nm) results in a decrease on the total backforce due to bubble expansion and, consequently, on the thermal instabilities. Opposite behavior was noted for the surfaces covered with the larger nanoparticles (d_p>40 nm), which presented an increase of the thermal instabilities due to the increment of the density of cavities within the range of active bubble nucleation sites and, consequently, on the total backforce due to bubble expansion inside the microchannel. Possible effects associated to variations of the surface tension due to the detachment of nanoparticles from the deposited layer into the fluid were evaluated by estimating the value of the surface tension according to the method of ??? assuming a volumetric concentration of 0.1%, the same value of the nanofluid used to produce the surface texture. Thus, much higher than the expected value for flow boiling of pure water on the nanostructured surface. From this analysis, it was founded a variation of the surface tension of only ???% compared to the value of pure water. Therefore, a possible effect of surface tension change on the instabilities was considered improbable..

4. CONCLUSIONS

Experiments were performed for flow boiling of DI-water inside microchannels with internal surfaces as commercially available and covered with nanoparticles of different sizes and materials. The experiments were focused on an analysis of the effect of nanocoating of the surfaces on the thermal instabilities, which intensity was evaluated based on the amplitude of the variation of the temperature of DI-water at the test section inlet. In general, thermal instability effects were minimized for the surfaces covered with nanoparticles smaller than 30 nm. Opposite behaviors were observed for the surfaces covered with nanoparticles larger than 40 nm.

The surface texture analysis through the PDSs indicated a reduction of the number of cavities within the range of active sites of bubble nucleation for the surfaces covered with the smaller nanoparticles (d_p<30 nm) in comparison with the bare tube. It is expected that the number of cavities within the range of active sites of bubble nucleation on the internal surface of the microchannel decreases and, therefore, causes a reduction of the total backforce against the flow associated to the bubbles expansion under confined conditions. For the surfaces covered with the larger nanoparticles (d_p>40 nm), practically none effect on the number of cavities within the range of active sites of bubble nucleation seemed to occur compared to the tube surface as commercially available, presenting even a slightly increase under certain conditions. In this case, it is expected that a suit increase in the number of cavities within the range of active sites of bubble nucleation results in an increment of the total backforce against the main flow associated to the bubbles expansion under confined conditions.

5. NOMECLATURE

ABN – Surface after boiling with nanofluids
BBN – Surface before boiling with nanofluids
d – Diameter, m
DC – Direct current
DI-water – Deionized water
G – Mass velocity, kg/m^{2}s
ID – Internal diameter
L – Length of the tube, m
p – Pressure, kPa
PSD – Power spectrum density
Q – Heat Flux, W/m^2
$r_{c,max}$ - Maximum radius of bubble nucleation, μm
$r_{c,min}$ - Minimum radius of bubble nucleation, μm
T – Temperature
V – Valve
ΔP – Differential pressure, kPa
ω – Volumetric concentration, %

6. ACKNOWLEDGEMENTS

The authors acknowledge the CNPq (National Council for Scientific and Technological Development, Brazil) for the grants given under Contracts Numbers 303852/2013-5 and 131082/2015-9, CAPES (Coordination for the Improvement of Higher Level Personal, Brazil) for the research grant given through the NANOBIOTEC research program and FAPESP (São Paulo Research Foundation, Brazil) for the scholarships and research grants under Contract Numbers 2011/13119-0, 2013/02869-4, 2016/16849-3 and 2016/09509-1. The authors also gratefully acknowledge Mr. José Roberto Bogni for the technical support on the development of the experimental facility and Prof. Renato Goulart Jasinevicius for the images obtained through the optical profiler.

7. REFERENCES

Abernethy, R. B. and Thompson, J. W., 1973. "*Handbook of uncertainty in gas turbine measurements*". Arnold Engineering Development Center, Arnold Air Force Station, Tenesse, USA.

Choi, S. U. S. and Eastman, J. A., 1995. "Enhancing thermal conductivity of fluids with nanoparticles". In *Proceedings of the ASME International Mechanical Engineering Congress & Exposition*. San Francisco, USA.

Collier, J and Thome, J. R. 1994. "*Convective boiling and condensation*". Third ed., Clarendo Press, Oxford.

Diao, Y. H., Liu, Y., Wang, R., Zhao, Y. H., Guo, I. and Tang, X., 2013. "Effects of nanofluids and nanocoatings on the thermal performance of an evaporator with rectangular microchannels". *International Journal of Heat and Mass Transfer*, Vol. 67, p. 183-193.

Forrest, E., Williams, E. and Buongiorno, J., Hu, L. W., Rubner, M. and Cohen, R., 2010. "Augmentation of nucleate boiling hat transter and critical heat flux using nanoparticle thin-film coatings". *International Journal of Heat and Mass Transfer*, Vol. 53, p. 58-67.

Kandlikar, S. G., Mizo, V. R., Cartwright, M. D. and Ikenze, 1997. "Bubble nucleation and growth characteristics in subcooled flow boiling of water". In *Proceedings of the ASME 32nd National Heat Transfer Conference*. Baltimore, USA.

Moreira, T. A., Nascimento, F. J. and Ribatski, G., 2017. "An investigation of the effect of nanoparticle composition and dimension on the heat transfer coefficient during flow boiling of aqueous nanofluids in small diameter channels (1.1 mm)". *Experimental Thermal and Fluid Science*, Vol. 89, p. 72-89 .

Souza, R. R., Passos, J. C. and Cardoso, E. M., 2014. "Influence of nanoparticle size and gap size on nucleate boiling using HFE7100". *Experimental Thermal and Fluid Science*, Vol. 59, p. 195-201.

Xu, L. and Xu, J., 2012. "Nanofluid stabilizes and enhances convective boiling heat transfer in a single microchannel". *International Journal of Heat Mass Transfer*, Vol. 55, p. 5673–5686.

Yu, L., Sur, A. and Liu, D., 2015. "Flow boiling heat transfer and two-phase flow instability of nanofluids in a minichannel". *Journal of Heat Transfer*, Vol. 137, p. 051502

Wen, D., Corr, M., Hu, X. and Lin, G., 2011. "Boiling heat transfer of nanofluids: The efect of surface modification". *International Journal of Thermal Sciences*, Vol. 50, p. 480-485.

8. RESPONSIBILITY NOTICE

The authors are the only responsible for the printed material included in this paper.